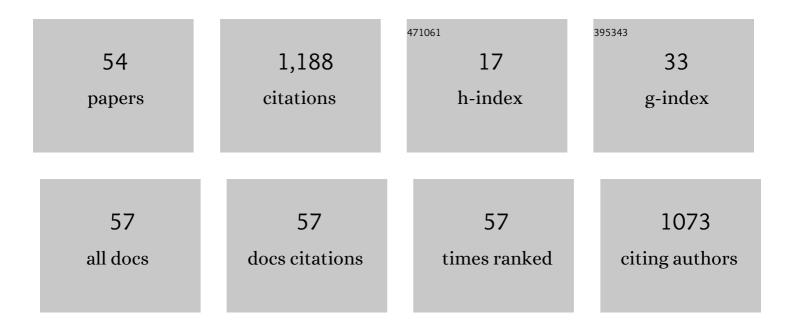
John Eberth

List of Publications by Year in descending order

Source: https://exaly.com/author-pdf/7685730/publications.pdf Version: 2024-02-01



IOHN FREDTH

| # | Article | IF | CITATIONS |
|----|---|-----|-----------|
| 1 | Fundamental role of axial stress in compensatory adaptations by arteries. Journal of Biomechanics, 2009, 42, 1-8. | 0.9 | 235 |
| 2 | Origin of axial prestretch and residual stress in arteries. Biomechanics and Modeling in Mechanobiology, 2009, 8, 431-446. | 1.4 | 162 |
| 3 | Mechanics of Carotid Arteries in a Mouse Model of Marfan Syndrome. Annals of Biomedical Engineering, 2009, 37, 1093-1104. | 1.3 | 76 |
| 4 | Importance of pulsatility in hypertensive carotid artery growth and remodeling. Journal of Hypertension, 2009, 27, 2010-2021. | 0.3 | 74 |
| 5 | Altered Hemodynamics in the Embryonic Heart Affects Outflow Valve Development. Journal of Cardiovascular Development and Disease, 2015, 2, 108-124. | 0.8 | 48 |
| 6 | Time course of carotid artery growth and remodeling in response to altered pulsatility. American Journal of Physiology - Heart and Circulatory Physiology, 2010, 299, H1875-H1883. | 1.5 | 44 |
| 7 | Consistent Biomechanical Phenotyping of Common Carotid Arteries from Seven Genetic, Pharmacological, and Surgical Mouse Models. Annals of Biomedical Engineering, 2014, 42, 1207-1223. | 1.3 | 43 |
| 8 | Acute mechanical effects of elastase on the infrarenal mouse aorta: Implications for models of aneurysms. Journal of Biomechanics, 2012, 45, 660-665. | 0.9 | 38 |
| 9 | A mechanical argument for the differential performance of coronary artery grafts. Journal of the Mechanical Behavior of Biomedical Materials, 2016, 54, 93-105. | 1.5 | 37 |
| 10 | The impact of flow-induced forces on the morphogenesis of the outflow tract. Frontiers in Physiology, 2014, 5, 225. | 1.3 | 33 |
| 11 | Evolving biaxial mechanical properties of mouse carotid arteries in hypertension. Journal of Biomechanics, 2011, 44, 2532-2537. | 0.9 | 28 |
| 12 | Mechanical and geometrical determinants of wall stress in abdominal aortic aneurysms: A computational study. PLoS ONE, 2018, 13, e0192032. | 1.1 | 25 |
| 13 | Multichannel Pulsed Doppler Signal Processing for Vascular Measurements in Mice. Ultrasound in Medicine and Biology, 2009, 35, 2042-2054. | 0.7 | 24 |
| 14 | Modeling and Validation of Automotive "Smart―Thermal Management System Architectures. , 0, , . | | 23 |
| 15 | Modelling carotid artery adaptations to dynamic alterations in pressure and flow over the cardiac cycle. Mathematical Medicine and Biology, 2010, 27, 343-371. | 0.8 | 23 |
| 16 | Comparative mechanics of diverse mammalian carotid arteries. PLoS ONE, 2018, 13, e0202123. | 1.1 | 23 |
| 17 | Geometric determinants of local hemodynamics in severe carotid artery stenosis. Computers in Biology and Medicine, 2019, 114, 103436. | 3.9 | 23 |
| 18 | Transforming Growth Factor Beta3 is Required for Cardiovascular Development. Journal of Cardiovascular Development and Disease, 2020, 7, 19. | 0.8 | 21 |

John Eberth

| # | Article | IF | CITATIONS |
|----|---|-----|-----------|
| 19 | Gold nanoparticles that target degraded elastin improve imaging and rupture prediction in an Angli mediated mouse model of abdominal aortic aneurysm. Theranostics, 2019, 9, 4156-4167. | 4.6 | 20 |
| 20 | Constitutive modeling of compressible type-I collagen hydrogels. Medical Engineering and Physics, 2018, 53, 39-48. | 0.8 | 18 |
| 21 | Comparison of Aortic Collagen Fiber Angle Distribution in Mouse Models of Atherosclerosis Using Second-Harmonic Generation (SHG) Microscopy. Microscopy and Microanalysis, 2016, 22, 55-62. | 0.2 | 16 |
| 22 | Contractile Smooth Muscle and Active Stress Generation in Porcine Common Carotids. Journal of Biomechanical Engineering, 2018, 140, . | 0.6 | 13 |
| 23 | Systemic delivery of targeted nanotherapeutic reverses angiotensin II-induced abdominal aortic aneurysms in mice. Scientific Reports, 2021, 11, 8584. | 1.6 | 13 |
| 24 | The perivascular environment along the vertebral artery governs segment-specific structural and mechanical properties. Acta Biomaterialia, 2016, 45, 286-295. | 4.1 | 11 |
| 25 | Targeted Gold Nanoparticles as an Indicator of Mechanical Damage in an Elastase Model of Aortic Aneurysm. Annals of Biomedical Engineering, 2020, 48, 2268-2278. | 1.3 | 11 |
| 26 | Removing vessel constriction on the embryonic heart results in changes in valve gene expression, morphology, and hemodynamics. Developmental Dynamics, 2018, 247, 531-541. | 0.8 | 10 |
| 27 | Advanced Engine Cooling – Components, Testing and Observations. IFAC Postprint Volumes IPPV / International Federation of Automatic Control, 2010, 43, 294-299. | 0.4 | 9 |
| 28 | Constitutive function, residual stress, and state of uniform stress in arteries. Journal of the Mechanics and Physics of Solids, 2012, 60, 1145-1157. | 2.3 | 8 |
| 29 | Chitosan and chitosan composites reinforced with carbon nanostructures. Journal of Alloys and Compounds, 2014, 615, S515-S521. | 2.8 | 7 |
| 30 | Null strain analysis of submerged aneurysm analogues using a novel 3D stereomicroscopy device. Computer Methods in Biomechanics and Biomedical Engineering, 2020, 23, 332-344. | 0.9 | 7 |
| 31 | Pulsatile Perfusion Bioreactor for Biomimetic Vascular Impedances. Journal of Medical Devices, Transactions of the ASME, 2018, 12, . | 0.4 | 6 |
| 32 | Evaluation of the Stress–Growth Hypothesis in Saphenous Vein Perfusion Culture. Annals of Biomedical Engineering, 2021, 49, 487-501. | 1.3 | 6 |
| 33 | Evaluation of heat propagation through poultry in a reduced computational ost model of contact cooking. International Journal of Food Science and Technology, 2012, 47, 1130-1137. | 1.3 | 5 |
| 34 | Design and Fabrication of a Three-Dimensional In Vitro System for Modeling Vascular Stenosis. Microscopy and Microanalysis, 2017, 23, 859-871. | 0.2 | 5 |
| 35 | Perfusion Tissue Culture Initiates Differential Remodeling of Internal Thoracic Arteries, Radial Arteries, and Saphenous Veins. Journal of Vascular Research, 2018, 55, 255-267. | 0.6 | 5 |
| 36 | Diet alters age-related remodeling of aortic collagen in mice susceptible to atherosclerosis. American Journal of Physiology - Heart and Circulatory Physiology, 2021, 320, H52-H65. | 1.5 | 5 |

John Eberth

| # | Article | IF | CITATIONS |
|----|--|----------------|--------------|
| 37 | The Association Between Curvature and Rupture in a Murine Model of Abdominal Aortic Aneurysm and Dissection. Experimental Mechanics, 2021, 61, 203-216. | 1.1 | 4 |
| 38 | Longitudinal histomechanical heterogeneity of the internal thoracic artery. Journal of the Mechanical Behavior of Biomedical Materials, 2021, 116, 104314. | 1.5 | 4 |
| 39 | Smallâ€diameter artery decellularization: Effects of anionic detergent concentration and treatment duration on porcine internal thoracic arteries. Journal of Biomedical Materials Research - Part B Applied Biomaterials, 2021, , . | 1.6 | 4 |
| 40 | Sintering of Chitosan and Chitosan Composites. , 2012, , . | | 3 |
| 41 | Reduced Smooth Muscle Contractile Capacity Facilitates Maladaptive Arterial Remodeling. Journal of Biomechanical Engineering, 2022, 144, . | 0.6 | 3 |
| 42 | On optimal defibrillating pulse synthesis. , 2011, , . | | 2 |
| 43 | A Novel Ex Ovo Banding Technique to Alter Intracardiac Hemodynamics in an Embryonic Chicken System. Journal of Visualized Experiments, 2016, , . | 0.2 | 2 |
| 44 | Myocardial TGFβ2 Is Required for Atrioventricular Cushion Remodeling and Myocardial Development. Journal of Cardiovascular Development and Disease, 2021, 8, 26. | 0.8 | 2 |
| 45 | Mechanics of ascending aortas from TCFβ-1, -2, -3 haploinsufficient mice and elastase-induced aortopathy. Journal of Biomechanics, 2021, 125, 110543. | 0.9 | 2 |
| 46 | Biofabrication of Dynamic, 3-Dimensional, In vitro Models of Disease. Microscopy and Microanalysis, 2015, 21, 619-620. | 0.2 | 2 |
| 47 | The Use of a Degradable Biomaterial to Regulate Fibrosis at the Implant-Host Interface. Microscopy and Microanalysis, 2016, 22, 1052-1053. | 0.2 | 1 |
| 48 | Design and Fabrication of a Three-Dimensional In Vitro Model of Vascular Stenosis. Microscopy and Microanalysis, 2016, 22, 1766-1767. | 0.2 | 1 |
| 49 | Brief communication: Maximum ingested bite size in captive western lowland gorillas (Gorilla gorilla) Tj ETQq1 1 | 0.78431 2.1 | 4 rgBT /Oved |
| 50 | Pathological Consequences of Altered Hemodynamics During Heart Valve Development. Microscopy and Microanalysis, 2016, 22, 1062-1063. | 0.2 | 0 |
| 51 | Molecular Consequences of Cardiac Valve Development as a Result of Altered Hemodynamics. Microscopy and Microanalysis, 2017, 23, 1330-1331. | 0.2 | 0 |
| 52 | Therapeutic Engineered Hydrogels Postpone Capsule Formation at the Host-Implant Interface. Microscopy and Microanalysis, 2017, 23, 1306-1307. | 0.2 | 0 |
| 53 | Integration of Heat Conduction Measurement Systems Into Engineering Technology Education. , 2005, , | | 0 |
| 54 | Dietâ€induced Vascular Remodeling Produces a Shift in Collagen Fiber Angle Distribution in a Mouse Model of Atherosclerosis. FASEB Journal, 2015, 29, 719.9. | 0.2 | 0 |